The MUSE Beam Line Calorimeter

Win Lin[1,2,3,*]

[1]Department of Physics and Astronomy, Rutgers, The State University of New Jersey, Piscataway, NJ 08855, USA
[2]Department of Physics and Astronomy, Stony Brook University, Stony Brook, NY 11794, USA
[3]Center for Frontiers in Nuclear Science, Stony Brook University, Stony Brook, NY 11794, USA

Abstract. The MUon proton Scattering Experiment (MUSE) at the PiM1 beam line of the Paul Scherrer Institute is simultaneously measuring the elastic scattering of electrons and muons from a liquid hydrogen target to extract the charge radius of the proton with both positive and negative beam polarities. In addition to providing precise data for addressing the proton radius puzzle, comparing the four scattering cross sections directly tests lepton universality, radiative corrections, and two-photon exchange effects for electrons and muons. In order to study radiative correction and get more precise incident lepton energy at the scattering vertex for the cross section measurements, MUSE uses a lead-glass calorimeter located at the downstream end of the beam line. This proceeding discusses the specifications and calibration process of the calorimeter detector. Data are compared to simulation to demonstrate the performance of the detector.

1 Introduction

The MUSE experiment was originally motivated by the proton radius puzzle, the discrepancy between the proton radius measured via muonic hydrogen spectroscopy versus electron hydrogen spectroscopy as well as electron-proton scattering [1, 2]. Since the puzzle was established, more measurements and re-analyses of existing data have been done. However, the results are inconsistent within the same type of measurements and analyses [3]. Hence, the proton radius is still a puzzle. MUSE is designed to perform an electron-proton and muon-proton elastic scattering simultaneously to provide more insight into the puzzle.

The MUSE experiment runs at the Paul Scherrer Institute in Villigen, Switzerland. It takes place at the PiM1 beamline with a mixed secondary beam of $e^{+/-}$, $\mu^{+/-}$ and $\pi^{+/-}$, at fluxes up to 3 MHz [4]. MUSE will be the first high precision muon-proton elastic scattering experiment. By measuring ep and μp scattering at the same time, and performing the experiment at both charge polarities, MUSE will provide a form factor comparison to other experiments in addition to the proton radius. A direct test of lepton universality will be done by comparing form factors obtained with ep vs. μp. Two-photon exchange contributions to ep and μp will be measured, and radiative corrections will be tested for both ep and μp scattering.

The kinematics of the MUSE experiment are given in Table 1. A description of the MUSE detector setup can be found in [5]. Because the MUSE setup covers a wide range of outgoing momenta and scattering angles without using a magnetic spectrometer common in traditional scattering experiments, the integration of the electron-proton scattering cross section will include a large fraction of the radiative tail. The experimental uncertainty is, therefore, sensitive to where the integration starts, which depends on the detector thresholds. To reduce the experimental uncertainty of the ep scattering cross section, MUSE uses a beamline lead-glass calorimeter located at downstream end of the apparatus to suppress high energy initial state radiation. High energy photons from initial state radiation are emitted in the forward direction. Applying a calorimeter energy cut significantly reduces the sensitivity to the radiative correction from experimental thresholds [6].

Table 1. MUSE Kinematic Coverage

Quantity	Coverage
Beam momenta	115, 160, 210 MeV/c
Scattering angle	20 - 100 degrees
Q^2 range for ep	0.0016 - 0.0820 (GeV/c^2)^2
Q^2 range for μp	0.0016 - 0.0799 (GeV/c^2)^2

2 Detector Description

The MUSE calorimeter consists of an 8×8 array of SF5 lead-glass crystal bars borrowed from the A2 experiment @ MAMI [7]. Each crystal is 4 cm wide $\times$ 4 cm tall $\times$ 30 cm long, covered by black shrink-wrap tubing. A schematic drawing of a detector bar is shown in Fig. 1. Each crystal channel uses a Hamamatsu R1355 photomultiplier for signal readout. The signals are delayed and sent to the Mesytec MCFD-16 constant fraction discriminators (CFDs) for timing readout [9] and the MQDC-32 charge to digital converter (QDCs) to integrate the signals for light output reconstruction [10].

*e-mail: win.lin@stonybrook.edu

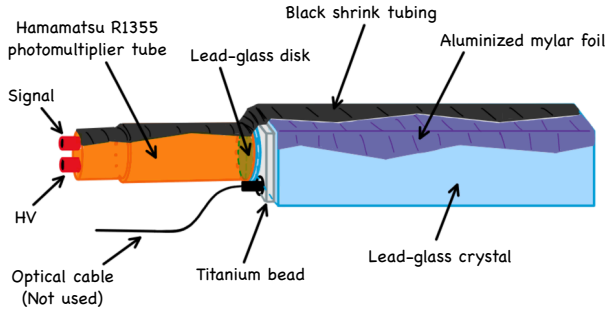

Figure 1. Schematic drawing of one detector bar [7, 8].

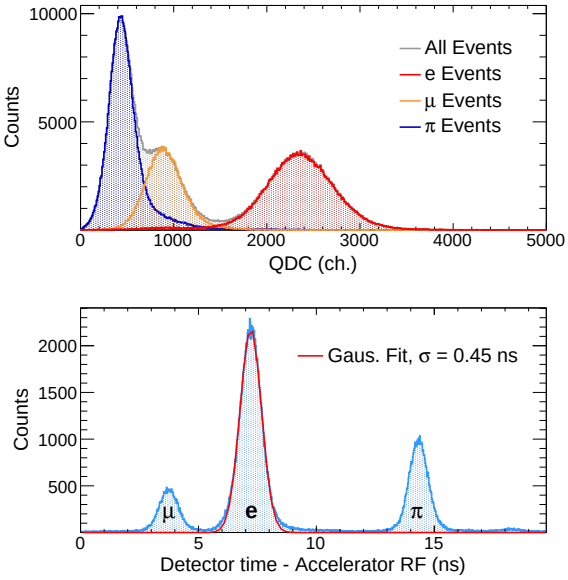

Figure 2. Example light output and timing spectra at a beam momentum of 160 MeV/c. Top: light output of the three particles in beam in unit of QDC channels. Bottom: (calorimeter time - accelerator RF time) modulo RF period (before walk correction).

The Molière radius and radiation length of lead glass is 2.578 cm and 1.265 cm respectively [11]. Hence, if particles hit the center of the crystal bar, the majority of the energy is contained within the crystal. However, particles can also clip corners or edges of the crystal. To reconstruct the light output of the detector, a 9-bar sum is used, where the light output of the channel with the highest QDC and the light output of its 8 surrounding neighbours are added together. Figure 2 shows an example of the reconstructed light output and timing spectra of the calorimeter. In the top plot, the 9-bar sums of the electron, muon, and pion beam events with momentum of 160 MeV/c are plotted, with electrons depositing the most energy, followed by muons, then pions, as expected at this momentum setting. The bottom plot shows the time difference between the calorimeter and the accelerator RF signals, modulo the accelerator RF period of 19.75 ns [4]. The timing peaks for the three particles are well separated, and the width of the timing peak indicates that the timing resolution of the calorimeter will be sufficient in distinguishing coincident hits from other particles in the beam. The timing resolution has about equal contributions from the accelerator pulse width and calorimeter timing.

3 Energy Response

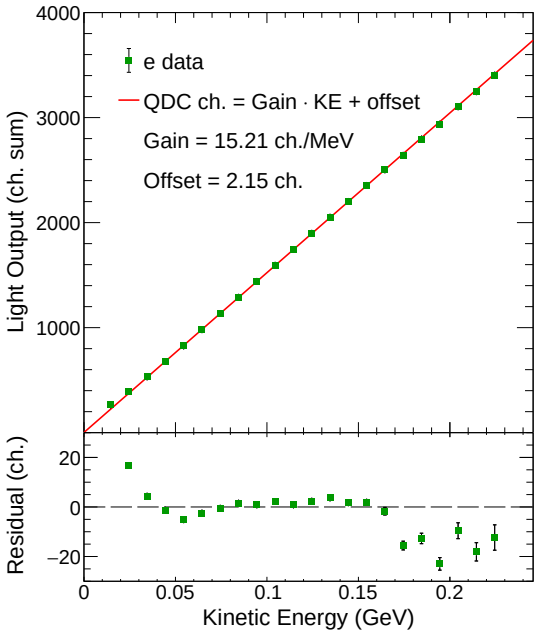

Figure 3. Light output vs. average incident beam electron energy.

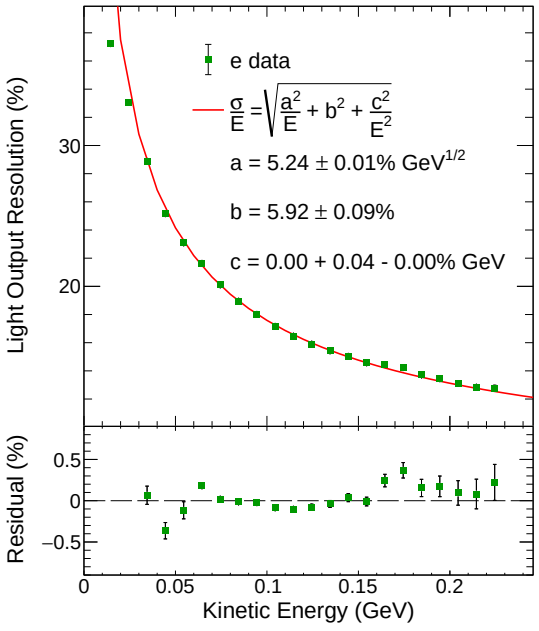

Figure 4. Resolution vs. average incident beam electron energy.

The gain of each channel of the calorimeter is calibrated using cosmic particles that uniformly illuminate the detector. Afterwards, beam data, which have more precisely known energies, are used to determine the light out-

put scale. Figure 3 shows the light output of the detector in units of QDC channels after the calibration as a function of the average incident electron energy, where the incident particle energy after energy losses in the upstream detectors and the target is estimated using simulation. The data are fitted with a first order polynomial to show linearity, and then the parameters of the fit are input to the simulation to model the detector response. Figure 4 shows the light output resolution of the detector as the incident electron energy varies. The data are fit with the typical light output resolution equation for calorimeters to quantify the detector performance. The stochastic contribution of the fit comes out to be about $5\%/\sqrt{E/\mathrm{GeV}}$, which is expected for a lead glass calorimeter [12]. Overall, the detector shows good linear light output response at our kinematics and reasonable light output resolution.

4 Simulation

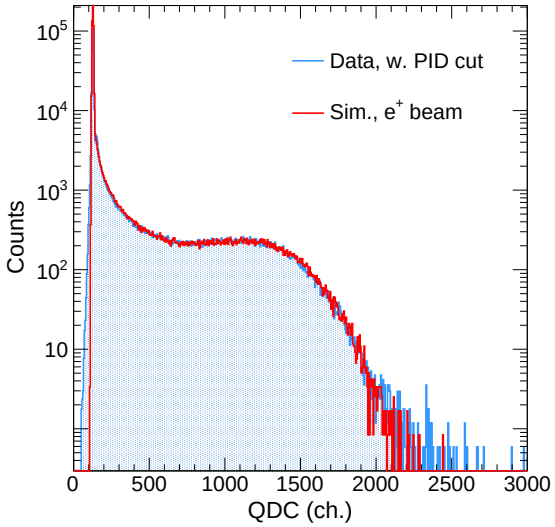

Figure 5. Comparison of a central crystal electron QDC spectrum from data vs. simulation for beam momentum of 110 MeV/c.

The MUSE experiment is simulated using Geant4. The detector response is derived from Cherenkov light production in the crystals. There are two modes to record the light output in the crystals. One is a fast mode where the light yield over the path in the crystal is integrated. The other is a more detailed simulation where the optical photons reaching the PMTs are counted. The simulated data are digitized and then analysed through the same analysis procedure applied to the data. In the digitization step, the simulated light output spectra of individual channels are tuned to match the data. There are three parameters involved: a gain parameter to model to QDC gain and efficiency of the readout, as well as two parameters, α and γ for fine tuning the resolution. The resolution is given by $\sqrt{\frac{\alpha^2}{E}+\frac{\gamma^2}{E^2}}$, with α and γ taking values similar to a and c from the light output response study discussed in Sec. 3. Since there are already some resolution effects in the simulation, α and γ are not exactly the same as a and c. Figure 5 compares the QDC spectrum of data with the fast-mode simulation for electrons at a beam momentum of 110 MeV/c, after the calibration of digitization. Data and simulation are well matched at the signal region by design.

After tuning the digitization, the overall detector response from simulation is compared to data. Figure 6 and Fig. 7 show preliminary results for the comparison of data and simulation for the calorimeter light output and resolution versus average incident electron energy. In this study, the simulation is tuned only using the 110 MeV/c data, yet data and simulation agree well especially at the region where the calorimeter energy cut will be applied. The agreement meets the experiment requirement (within 2 MeV) [6]. More tuning and further development of the simulation development are ongoing.

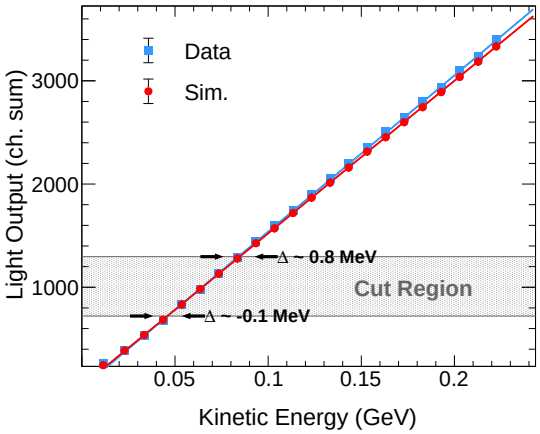

Figure 6. Comparison between data and simulation for calorimeter light output vs. average incident beam electron energy.

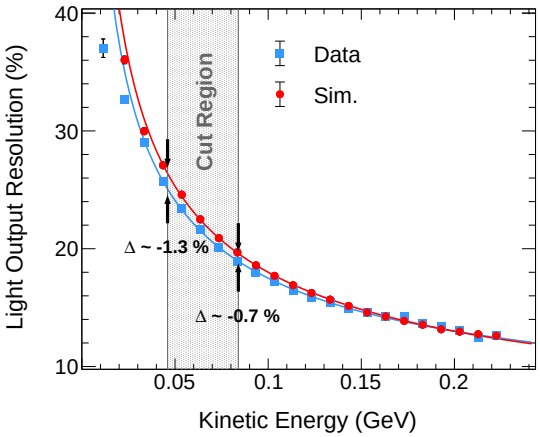

Figure 7. Comparison between data and simulation for calorimeter light output resolution vs. average incident beam electron energy.

5 Photon Reconstruction

The calorimeter is used to veto the scattering events with the high energy forward going photons. These events have

incoming particle timing in the BH detector, but leave no signals in the BM detector. Using this information, the photon events are reconstructed as shown in Figure 8, where the QDC spectrum for electron scattering events within experimental acceptance at 160 MeV/c is compared for data and simulation. MUSE scattering data and simulation are independently blinded at the current stage of the analysis [13]. For this reason, it is not expected that the data and simulation agree exactly. Nevertheless, data and simulation show similar behaviour for the high energy photon peak in this preliminary study. The nominal energy cut ($E_\gamma < 40\% p_0 c$, where p_0 is the beam electron momentum), shown by the black dashed line, will effectively remove the high-photon-energy events. The differences in the lower photon-energy events are likely due to the different threshold settings in the data vs. in the simulation.

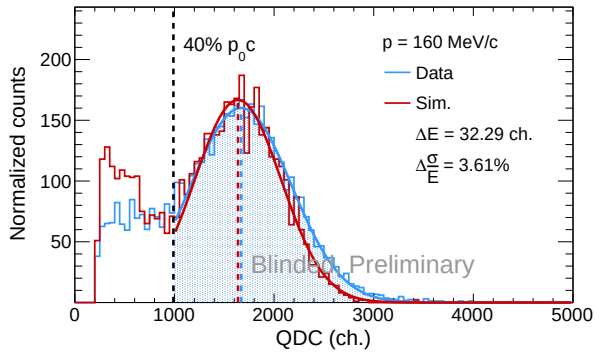

Figure 8. Preliminary reconstructed photons from scattering electron events at a beam momentum of 160 MeV/c (data and simulation are normalized by the number of events).

6 Discussion and Summary

The MUSE beamline calorimeter has a good linear light output response and resolution as shown above. Preliminary comparisons of data to simulation show that the detector performance is as expected and reasonably well understood. Photon events from the initial state radiation of ep scattering are successfully reconstructed. The detector will be able to remove events with high energy photons and limit experimental uncertainties from radiative corrections. Current calculations indicate that the radiative corrections and their uncertainties will be reduced by factors of about 2.5 to 5.5 with the nominal calorimeter energy cut, limiting uncertainties in radiative corrections from instrumental effect to 0.22% - 0.33% [6]. MUSE will vary the energy cut of the calorimeter to test its effect on the cross section, testing the radiative corrections. Hence, the beamline calorimeter is a powerful tool that MUSE will use to test radiative correction for both electrons and muons. Analysis and simulation work for the calorimeter is ongoing. More detailed description of the detector will be found in [14].

7 Acknowledgements

The MUSE experiment is supported by the U.S. National Science Foundation, in particular award PHY-2209348 to Rutgers University, the U.S. Department of Energy, the Paul Scherrer Institute, and the US-Israel Binational Science Foundation.

References

[1] R. Pohl et al., The size of the proton, Nature **466**, 213–216 (2010). 10.1038/nature09250
[2] A. Antognini et al., Proton structure from the measurement of 2S-2P transition frequencies of muonic hydrogen, Science **339**, 417 (2013). 10.1126/science.1230016
[3] Bernauer, J. C., The proton radius puzzle – 9 years later, EPJ Web Conf. **234**, 01001 (2020). 10.1051/epjconf/202023401001
[4] E. Cline et al., Characterization of muon and electron beams in the Paul Scherrer Institute PiM1 channel for the MUSE experiment, Physical Review C **105** (2022). 10.1103/physrevc.105.055201
[5] E. Cline et al., MUSE: The MUon Scattering Experiment, SciPost Phys. Proc. p. 023 (2021). 10.21468/SciPostPhysProc.5.023
[6] L. Li et al., Instrumental uncertainties in radiative corrections for the MUSE experiment, Eur. Phys. J. A **60**, 8 (2024), 2307.06417. 10.1140/epja/s10050-023-01215-0
[7] D. Eyl, Ph.D. thesis, Johannes Gutenberg-Universität Mainz (1993), mainz, Univ., Diss., 1993
[8] C. Nestler (2023), unpublished Semester Thesis
[9] Mesytec GmbH & Co. KG. MCFD-16 16 channel CFD with fast amplifier and pattern processing, accessed: 8-18-2023, http://www.mesytec.com/products/datasheets/MCFD-16.pdf
[10] Mesytec GmbH & Co. KG. MQDC-32 fast 32 channel VME charge integrating ADC, accessed: 8-18-2023, http://www.mesytec.com/products/datasheets/MQDC-32.pdf
[11] R.L. Workman et al. (Particle Data Group), Review of Particle Physics, PTEP **2022**, 083C01 (2022). 10.1093/ptep/ptac097
[12] M. Tanabashi et al. (Particle Data Group), Review of particle physics, Phys. Rev. D **98**, 030001 (2018). 10.1103/PhysRevD.98.030001
[13] J.C. Bernauer et al., Blinding for precision scattering experiments: The MUSE approach as a case study (2023), 2310.11469, https://arxiv.org/abs/2310.11469
[14] W. Lin et al., The MUSE beamline calorimeter (2024), 2408.13380, https://arxiv.org/abs/2408.13380